Electronic Supplementary Information

Fluoride-free synthesis of high-silica CHA-type aluminosilicates by seed-assisted aging treatment for starting gel

Ryota Osuga,[a*] Mizuho Yabushita,[b] Takeshi Matsumoto,[c] Masato Sawada,[c] Toshiyuki Yokoi,[c] Kiyoshi Kanie,[a,d] and Atsushi Muramatsu [a,d*]

a Institute of Multidisciplinary Research for Advanced Materials, Tohoku University, Sendai, Miyagi 980-8577, Japan

b Department of Applied Chemistry, School of Engineering, Tohoku University, 6-6-07 Aoba, Aramaki, Aoba-ku, Sendai, Miyagi 980-8579, Japan

c Institute for Innovative Research, Tokyo Institute of Technology, 4259 Nagatsuta, Midori-ku, Yokohama 226-8503, Japan

d International Center for Synchrotron Radiation Innovation Smart, Tohoku University, 2-1-1 Katahira, Aoba-ku, Sendai, Miyagi 980-8577, Japan

Author information

Corresponding Authors

*E-mail; ryota.osuga.d4@tohoku.ac.jp (R. O.)

*E-mail; mura@tohoku.ac.jp (A. M.)

Table of Contents

Experimental

1. Synthesis of SSZ-13.

SSZ-13(10) (**CHA**, Si/Al = 10) was synthesized via hydrothermal synthesis using a previously reported method.[S1] NaOH (FUJIFILM Wako Pure Chemical) and $Al(OH)_3$ (Sigma-Aldrich) were dissolved in a 20 wt% *N*,*N*,*N*-trimethyladamantanammonium hydroxide (TMAdaOH, Sachem) aqueous solution. Amorphous silica (Cabosil-M5) was then added to the solution such that the gel composition was $1.0SiO_2$: $0.1Al(OH)_3$: 0.2TMAdaOH : 0.2NaOH : $30H_2O$. The prepared gel was hydrothermally treated at 170 °C for 5 days by tumbling at 40 rpm. The as-prepared sample was calcined at 600 °C for 6 h. The sample was then ion-exchanged using a 2.5 M NH_4NO_3 aqueous solution at 80 °C for 3 h twice to obtain the NH_4^+-form sample, which was further converted to the H^+-form of SSZ-13 by calcination at 600 °C for 3 h.

2. Synthesis of high-silica **CHA**-type aluminosilicates.

Starting gels for high-silica **CHA**-type aluminosilicates were prepared via the same procedure asSSZ-13(10) using TMAdaOH as an OSDA. The Si/Al molar ratio of the gels was varied in the range from 50 to 500. Before the hydrothermal treatment, SSZ-13(10) (2 wt% to SiO_2) was added to the starting gel; the gel was then stirred at room temperature for 24 h. The starting gels were hydrothermally treated at 170 °C for 2 days by tumbling at 40 rpm. Afterwards, the ion-exchange procedures were performed in the same manner as SSZ-13(10). The obtained samples were designated as CHA(*X*), where *X* is the Si/Al molar ratio in the starting gel.

3. Characterization.

The synthesized zeolites were characterized using various techniques. The crystal structure was investigated by powder X-ray diffraction (XRD; Ultima IV, Rigaku, Cu Kα radiation (40 kV, 40 mA)) analysis. The Si/Al ratio was determined by inductively coupled plasma atomic emission spectroscopy (ICP-AES; SPECTRO ARCOS, AMETEK) measurements. The number of organic-structure-directing agents was determined by a thermogravimetry-differential thermal analysis (TG-DTA) measurement (RigakuThurmo plus EVO II, Rigaku). The specific surface area and micropore volume were elucidated using N_2 adsorption–desorption measurements (BELSORP-mini, MicrotracBEL) after pretreatment (BELPREP-vac III, MicrotracBEL) of the samples at 400 °C for 1 h under reduced pressure. The Brunauer–Emmett–Teller (BET) specific surface area was calculated from the adsorption data in the relative pressure (p/p_0) range from 0.01 to 0.1. The micropore volume was estimated by the *t*-plot method. Morphological observations were conducted by field-emission scanning electron microscopy (FE-SEM; S-5200, Hitachi). Electrospray ionization mass (ESI-MS) spectroscopy was performed in negative-ion

mode using a TripleTOF 5600 System (AB SCIEX). ESI-MS spectra were acquired using an ion-spray voltage of −4.5 kV, curtain gas pressure of 10 psi, nebulizer gas pressure of 15 psi, interface heater temperature of 200 °C, and flow rate of 10 μL min^{-1}. High-resolution ^{27}Al and ^{29}Si MAS NMR spectra were recorded on a JEOL ECA-600 spectrometer (14.1 T) equipped with an additional 1 kW power amplifier. The chemical shifts of ^{27}Al and ^{29}Si were referenced to $AlNH_4(SO_4)_2 \cdot 12H_2O$ at −0.54 ppm and dimethylpolysiloxane at −34.12 ppm, respectively. The samples were spun at 15 kHz using a 4 mm ZrO_2 rotor. The number and strength of Brønsted acid sites were estimated using NH_3 temperature-programmed desorption (NH_3-TPD) measurements, which were performed using a BELCAT (MicrotracBEL) equipped with a quadrupole mass spectrometer (Q-MS; BELMass, MicrotracBEL). Before the measurements, each sample was pretreated at 500 °C for 30 min under He flow at 30 mL min^{-1}. The temperature range, ramp rate, and He flow rate for the TPD program were 100–700 °C, 10 °C min^{-1}, and 30 mL min^{-1}, respectively. The pretreated samples were exposed to 10.3 vol% NH_3/He gas at 100 °C for 30 min, and then physically adsorbed NH_3 was removed under flowing He (30 mL min^{-1}) at 100 °C for 30 min. Fourier transform infrared (FT-IR) spectra were obtained using a JASCO FT/IR-4600 spectrometer equipped with a mercury-cadmium-telluride detector. All spectra were collected as averages of 64 scans with a resolution of 4 cm^{-1}. Self-supporting disks of each sample (20 mm diameter, 30 mg) were placed in a quartz cell connected to a conventional closed gas-circulation system. The samples were pretreated at 450 °C for 1 h under evacuation to remove the adsorbed species, and IR spectra were recorded at 25 °C.

4. Methanol-to-olefins (MTO) reaction.

The MTO reaction was performed using a fixed-bed reactor connected to an online gas-chromatograph (GC-2014, Shimadzu) equipped with a HP-PLOT/Q capillary column and a flame ionization detector. The 50/80 mesh zeolite pellets without a binder were placed in a 6 mm quartz tubular flow reactor. The pretreatment was conducted at 500 °C for 30 min under flowing air (20 mL min^{-1}). After the pretreatment, the reactor was cooled to 350 °C and the MTO reaction was started. The pressure of methanol was set at 5 kPa with Ar gas as the carrier; the weight-to-feed ratio (*W/F*) for methanol was 68 g h mol^{-1}. The product stream was analyzed using a system that automatically injected the product into a gas chromatograph connected directly to the outlet of the reactor via a heated transfer line.

Calculation methods

1. Solid yield for synthesis.

   The solid yield was calculated using:

$$Solid\ yield\ [\%]\ = \frac{Weight\ of\ the\ calcined\ zeolite}{Weight\ of\ SiO2\ and\ Al2O3\ in\ the\ starting\ gel} \times 100$$

(Eq. S1)

2. Conversion and selectivity in MTO reaction.

   The conversion and selectivity were calculated according to Eqs. S2 and S3:

$$Conversion\ of\ methanol\ [\%]\ = 1 - \frac{Amount\ of\ methanol\ (in\ reacted\ gas)}{Amount\ of\ detected\ compounds\ (in\ reacted\ gas)} \times 100$$

(Eq. S2)

$$Product\ selectivity\ [\%]\ = \frac{Amount\ of\ the\ target\ product}{Amount\ of\ detected\ products\ (in\ reacted\ gas)} \times 100$$

(Eq. S3)

Table S1 Comparison of Si/Al ratios and synthetic conditions of this work and those of previous studies involving synthesis of high-silica **CHA**-type aluminosilicates.

Authors	Si/Al molar ratio	Syntheis method	Fluoride	Seed	Publication year	Ref.
Zones *et al.*	≤ 14	Hydrothermal synthesis	Not used	Not used	1985	[S2]
Díaz-Cabañas *et al.*	∞	Hydrothermal synthesis	Used	Not used	1998	[S3]
Zhu *et al.*	≤ 67	Hydrothermal synthesis	Not used	Used	2008	[S4]
Wu *et al.*	≤ 61	Hydrothermal synthesis	Not used	Not used	2014	[S5]
Kubota *et al.*	≤ 146	Hydrothermal synthesis	Not used	Used	2016	[S6]
Zhu *et al.*	≤ 140	Acid post-treatment	-	-	2019	[S7]
Li *et al.*	≤ 42	Steam-assisted crystallization	Not used	Not used	2019	[S8]
Al Jabri *et al.*	≤ 182	Dry gel conversion	Used	Used	2019	[S9]
Osuga *et al.*	≤ 156	Hydrothermal synthesis	Not used	Used	This work	

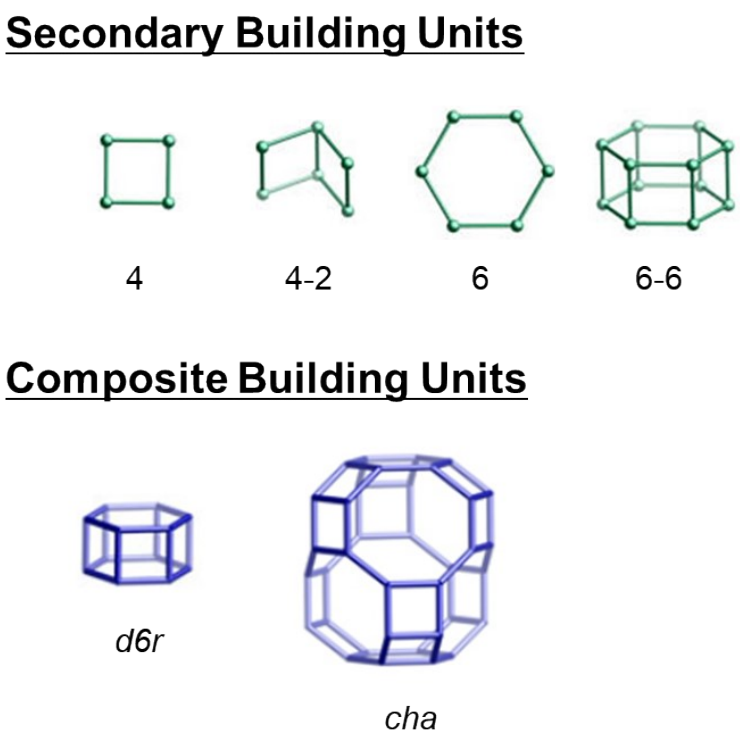

Fig. S1 Building units for **CHA**-type frameworks.[S10]

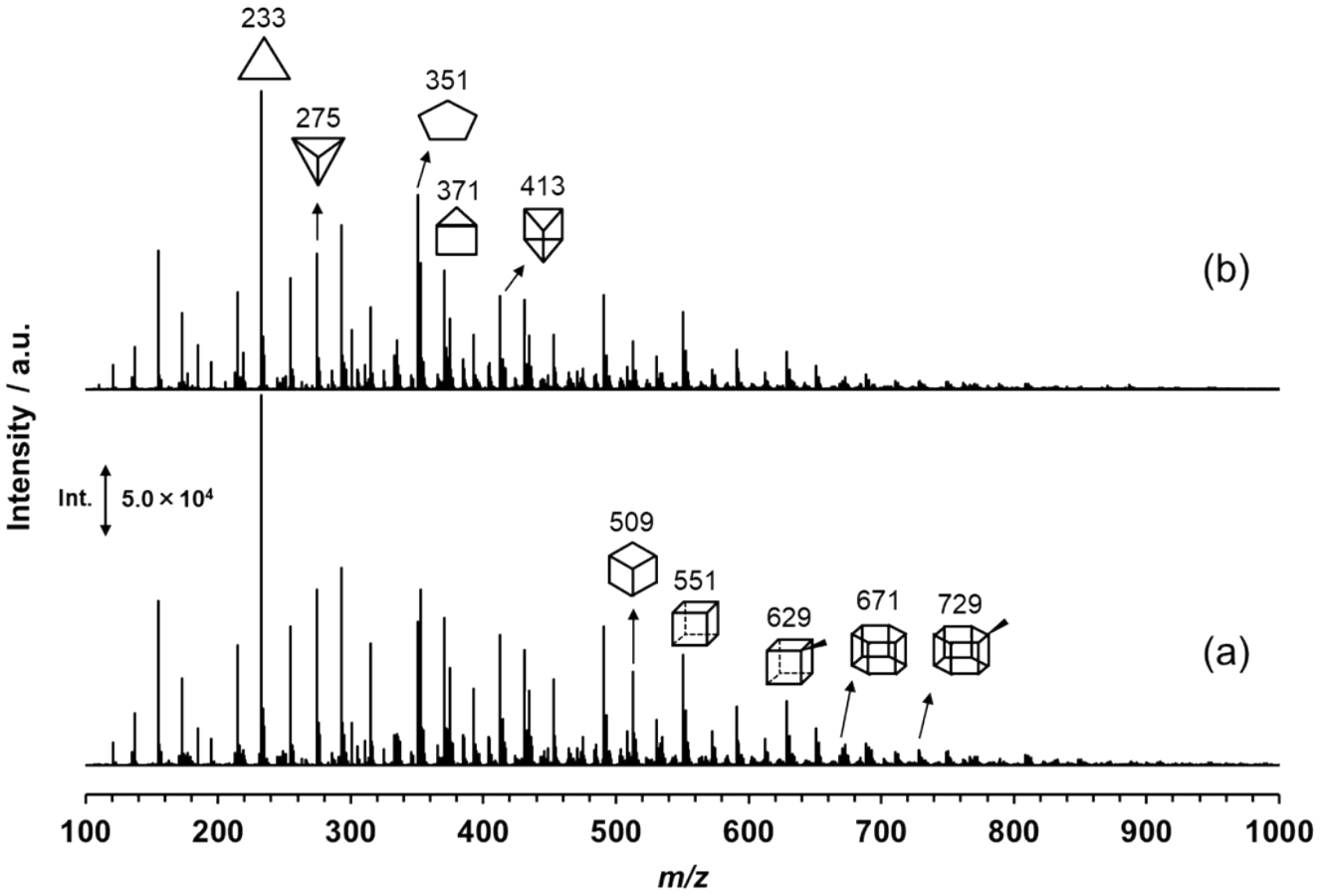

Fig. S2 ESI-MS spectra of liquid phase of starting gels prepared using gel with same composition as that used to prepare CHA(200): (a) with seed crystal and (b) without seed crystal. The spectra were normalized on the basis of the peak of $TMAda^+$ (*m/z* = 194). Numbers at the chemical structures indicate their *m*/*z*.

Table S2 Comparison for intensity of ESI-MS spectra of dissolved even numbered-ring species in the starting gels.[a]

Starting gels	Normalized intensity in ESI-MS spectra ($\times 10^4$)				
					
With seed crystal	6.5	7.7	4.5	1.5	1.1
Without seed crystal	3.3	5.4	2.3	0.3	0.5

[a]These values correspond to Fig. S2.

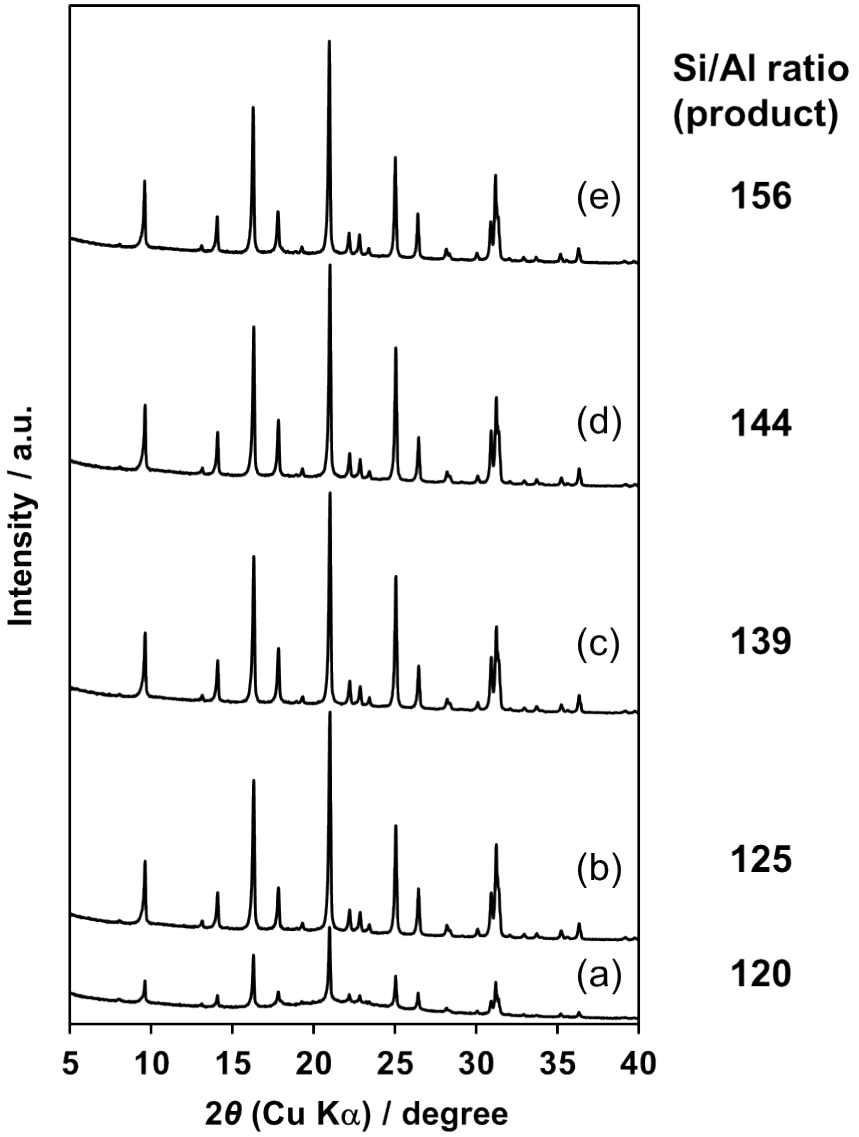

Fig. S3 XRD patterns for synthesized **CHA**-type zeolites (as-prepared) with different aging times: (a) 0, (b) 3, (c) 6, (d) 12 and (e) 24 h (CHA(300)). The Si/Al ratios were estimated by ICP-AES.

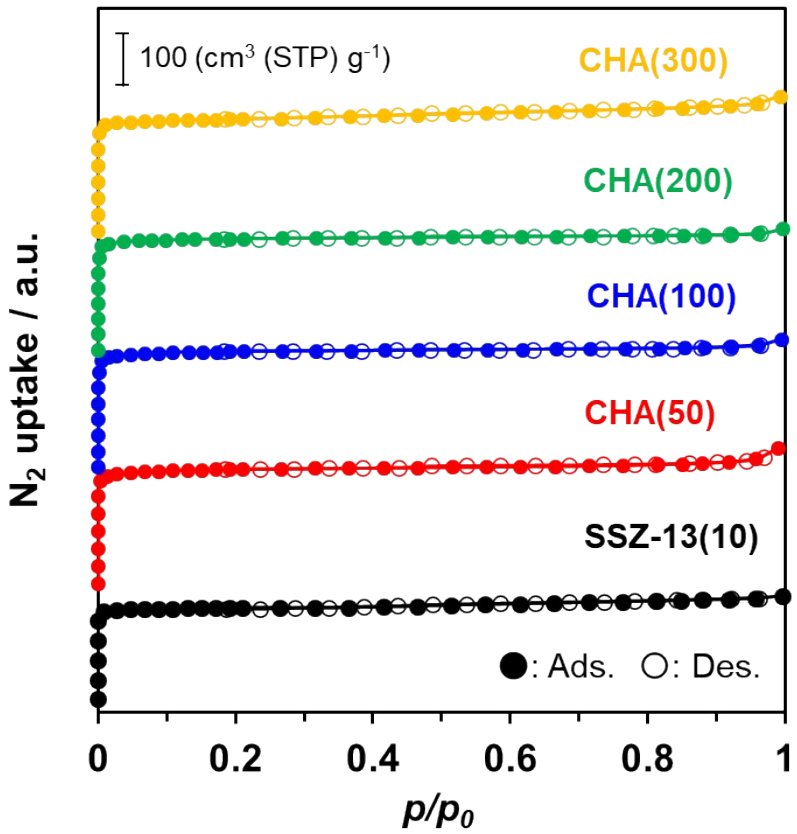

Fig. S4 N_2 adsorption–desorption isotherms for synthesized **CHA**-type aluminosilicates.

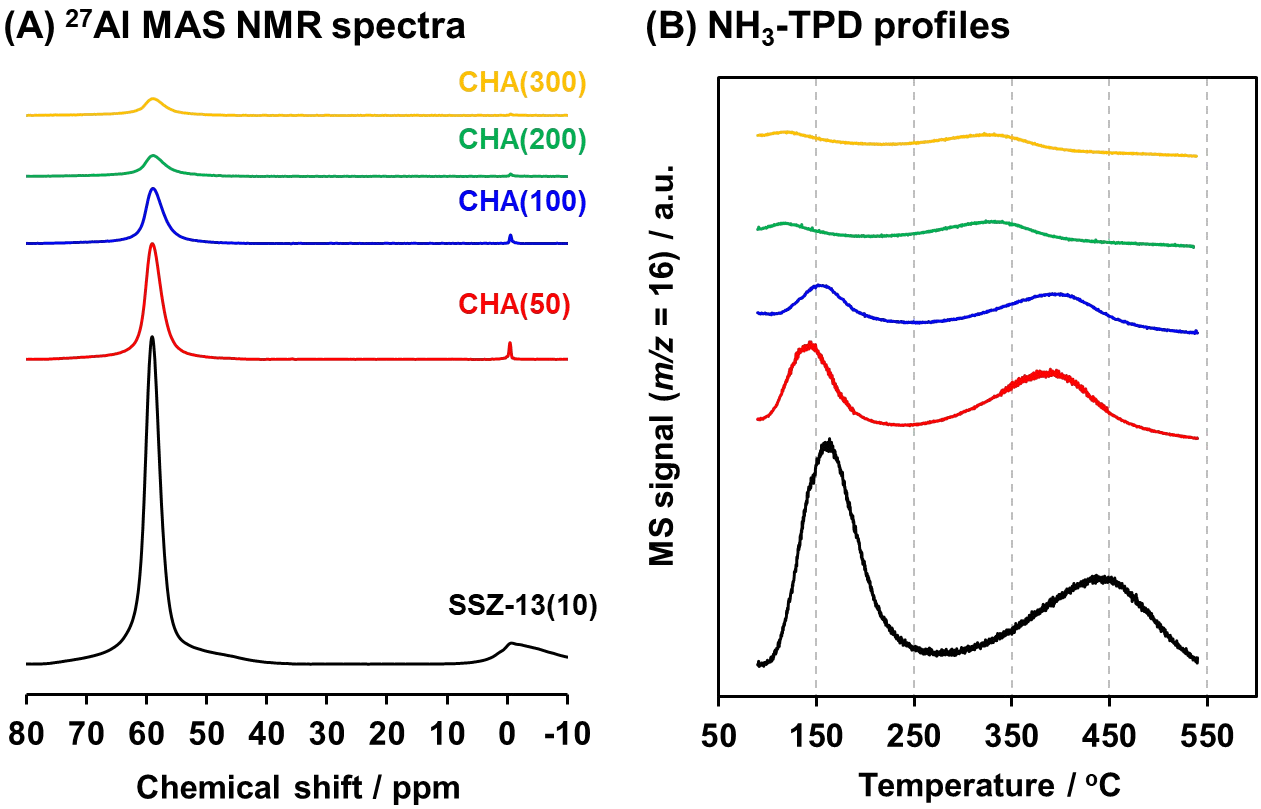

Fig. S5 (A) ^{27}Al MAS NMR spectra and (B) NH_3-TPD profiles for each sample.

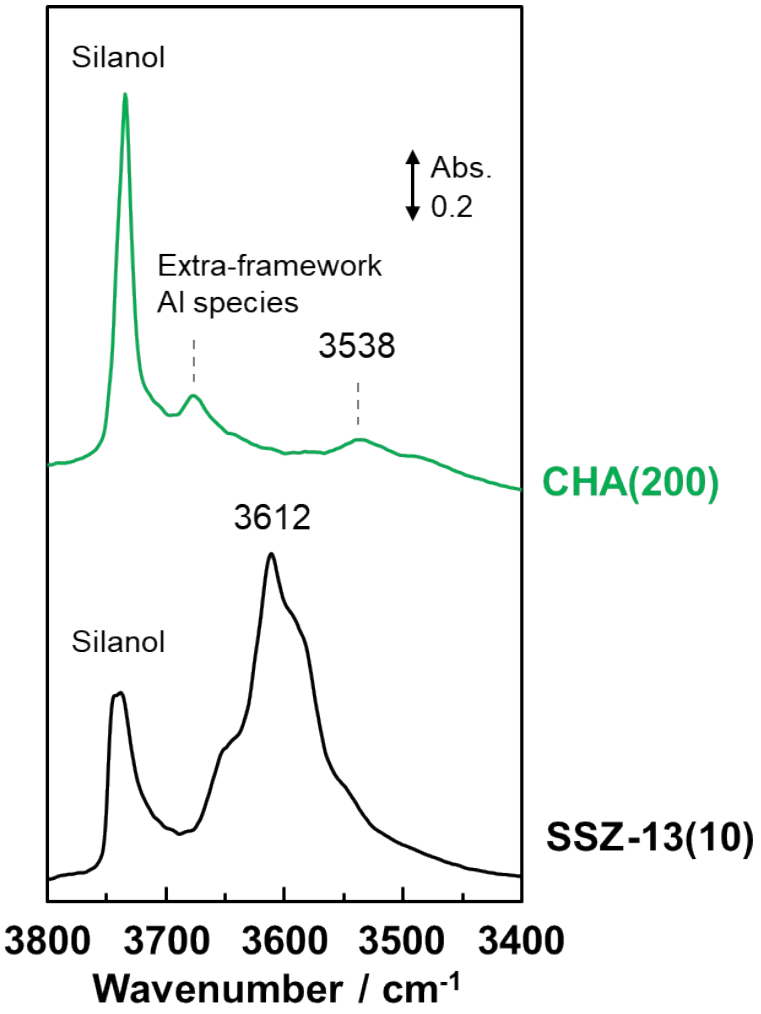

Fig. S6 FT-IR spectra of SSZ-13(10) and CHA(200) at 25 °C.

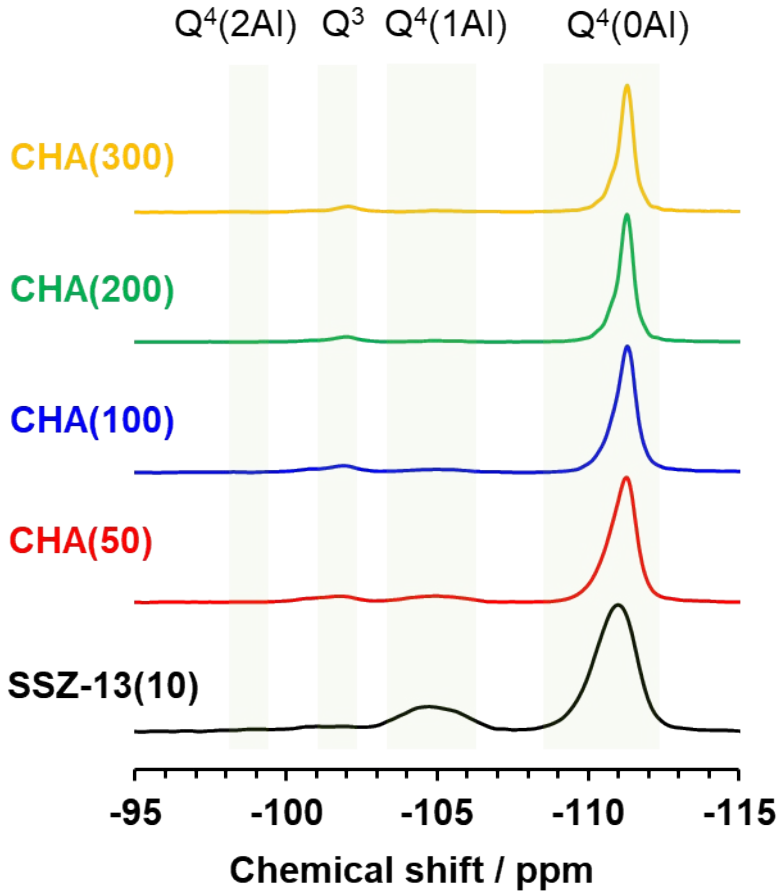

Fig. S7 ^{29}Si MAS NMR spectra of each sample.

Table S3 Quantitative analysis for ^{29}Si MAS NMR measurements.[a]

Sample	Integrated intensity				Q^3/Q^4
	$Q^4(0Al)$	$Q^4(1Al)$	$Q^4(2Al)$	Q^3	
SSZ-13(10)	6.50	1.95	0.41	0.26	0.05
CHA(50)	7.82	0.80	0	0.67	0.08
CHA(100)	8.26	0.42	0	0.72	0.08
CHA(200)	7.55	0.13	0	0.52	0.07
CHA(300)	7.11	0.08	0	0.46	0.06

[a]Examined via deconvolution of ^{29}Si MAS NMR spectrum shown in Fig. S7.

Table S4 Catalytic performance of **CHA**-type aluminosilicates in MTO reaction at initial stage.

Samples	Conversion (C-atom%)	Product selectivity (C-atom%)				
		$C_{2=}$	$C_{3=}$	$C_{4=}$	Over C_{5s}	Paraffins
SSZ-13(10)	>99	14	23	14	6	43
CHA(50)	>99	34	36	14	7	9
CHA(100)	>99	37	38	14	7	4
CHA(200)	>99	41	38	14	5	2
CHA(300)	>99	40	37	13	8	2

Reaction conditions: 100 mg catalyst, 5 vol% methanol in Ar gas, W/F_{MeOH} = 68 g h mol^{-1}, TOS = 10 min.

Supplementary references

[S1] R. Osuga, T. Yokoi and J. N. Kondo, *J. Catal.*, 2019, **371**, 291–297.

[S2] S. I. Zones, *US Pat.*, 1985, 4,544,538

[S3] M. J. Díaz-Cabañas, P. A. Barrett and M. A. Camblor, *Chem. Commun.*, 1998, 1881–1882.

[S4] Q. Zhu, J. N. Kondo, R. Ohnuma, Y. Kubota, M. Yamaguchi and T. Tatsumi, *Microporous Mesoporous Mater.*, 2008, **112**, 153–161.

[S5] L. Wu and E. J. M. Hensen, *Catal. Today*, 2014, **235**, 160–168.

[S6] Y. Kubota, S. Inagaki and T. Fukuoka, JP Pat., P2016-169118A, 2016.

[S7] M. Zhu, L. Liang, H. Wang, Y. Liu, T. Wu, F. Zhang, Y. Li, I. Kumakiri, X. Chen and H. Kita, *Ind. Eng. Chem. Res.*, 2019, **58**, 14037–14043.

[S8] Y. Li, R. Liu, Q. Guo, H. Bian, A. Lan, X. Li, P. Han and T. Dou, *J. Porous Mater.*, 2019, **26**, 1879–1888.

[S9] H. Al Jabri, K. Miyake, K. Ono, M. Nakai, Y. Hirota, Y. Uchida, M. Miyamoto and N. Nishiyama, *Microporous Mesoporous Mater.*, 2019, **278**, 322–326.

[S10] C. Baerlocher and L. B. McCusker, Database of Zeolite Structures, http://www.iza-structure.org/databases/, (accessed July 2022).